

# Layer-by-Layer Ultrathin Films of Azobenzene-Containing Polymer/Layered Double Hydroxides with Reversible Photoresponsive Behavior

Jingbin Han,<sup>†</sup> Dongpeng Yan,<sup>†</sup> Wenying Shi,<sup>†</sup> Jing Ma,<sup>‡</sup> Hong Yan,<sup>†</sup> Min Wei,<sup>\*,†</sup> David G. Evans,<sup>†</sup> and Xue Duan<sup>†</sup>

State Key Laboratory of Chemical Resource Engineering, Beijing University of Chemical Technology, Beijing 100029, P. R. China, and Mesoscopic Chemistry of MOE, Nanjing University, Nanjing 210093, P. R. China

Received: December 01, 2009; Revised Manuscript Received: March 31, 2010

We report the preparation of a reversible photoresponsive ultrathin film containing a photoactive azobenzene polymer poly{1-4[4-(3-carboxy-4-hydroxyphenylazo)benzenesulfonamido]-1,2-ethanediyl sodium salt} (PAZO) and exfoliated layered double hydroxide (LDH) nanosheets using a layer-by-layer (LBL) self-assembly technique. Alternate irradiation with UV and visible light ( $\lambda > 450$  nm) results in a reversible switching between the trans isomer and the cis-rich photostationary state of the azobenzene group with concomitant significant changes in film color. Fluorescence polarization measurements indicated that the orientation of the azobenzene chromophores in the LDH matrix undergoes a reversible realignment during the photoisomerization processes. Photoisomerization induced by alternate UV and visible light irradiation was accompanied by reversible morphological changes of the LBL film, observable by atomic force microscopy (AFM). Molecular dynamics (MD) studies demonstrated that the LDH monolayers allow sufficient free space for the PAZO to undergo isomerization of its azobenzene chromophores. The reversible photoalignment of PAZO was also followed by MD simulations, and the results are in reasonable agreement with the experimental findings, further validating the configurational and orientational changes proposed for PAZO during the reversible photoprocess. It has been demonstrated that the host (LDH nanosheet)–guest (PAZO) interactions are key factors in determining the reversible photoresponsive performances of the film, since the comparative pristine PAZO film shows no such properties. Therefore, the incorporation of a photoactive moiety within the inorganic nanosheets of LDH by the LBL technique provides an attractive and feasible methodology for creating novel light-sensitive materials and devices with potential read–write capabilities.

## Introduction

The photoinduced cis–trans isomerization of azobenzene and its derivatives is a well-known photochemical phenomenon<sup>1</sup> which has been extensively studied for the past 50 years, since these materials present many interesting features and their applications range from electronics to biomedicine. Recently, considerable research efforts have been directed toward the development of simple protocols for the preparation of azobenzene-containing thin films with controlled architecture; these are considered to be very promising materials for optical information storage,<sup>2</sup> light switching,<sup>3</sup> sensors,<sup>4</sup> variable wettability,<sup>5</sup> liquid crystal alignment,<sup>6</sup> and nonlinear devices.<sup>7</sup> It is known that the microenvironment around azobenzene chromophores plays a crucial role in the photoisomerization process.<sup>8</sup> Azobenzenes have been included in the cavity of amphiphilic cyclodextrins,<sup>9</sup> embedded in hydrophobic copolymer micelles,<sup>10</sup> or incorporated with inorganic clays,<sup>11</sup> in order to obtain the sufficient free volume necessary for the isomerization of the azobenzene groups. Up to now, a large variety of spin-casting,<sup>12</sup> Langmuir–Blodgett (LB) deposition,<sup>13</sup> and layer-by-layer (LBL) electrostatic self-assembly<sup>14</sup> techniques have been employed to construct azobenzene-containing solid films, among which the LBL technique has attracted considerable interest because of its accurate control over film thickness, simplicity, and low-

cost equipment as well as the lack of dependence of film deposition on the type, size, and morphology of a substrate.

Most reports of azobenzene films fabricated by the LBL method have been based on the deposition of oppositely charged organic polycations and polyanions, either of which can contain the azobenzene chromophores. In this kind of assembly of polyelectrolyte multilayers, the penetration between adjacent polymers and strong  $\pi$ – $\pi$  stacking of azobenzene chromophores may lead to a lack of sufficient free volume for the azobenzene groups to undergo isomerization and lead to irreversibility or low efficiency of the process. This is the main bottleneck in developing optical devices with superior optical properties based on the isomerization of azobenzene. A potential solution to this problem would be the substitution of one polymer (polycation or polyanion) by a rigid two-dimensional (2D) inorganic matrix. It can be expected that the severe interpenetration of the azobenzene groups may be restrained by the isolating effect of the 2D inorganic matrix, and the formation of an ordered distribution and alignment of the azobenzene groups with sufficient available free space in the interlayer galleries between the inorganic sheets should facilitate their photoisomerization. However, electrostatic LBL assembly of an azobenzene-bearing polyelectrolyte and oppositely charged inorganic nanosheets has not yet been reported.

Layered double hydroxides (LDHs) are layered anionic clays generally expressed by the formula  $[M_{1-x}^{2+}M_x^{3+}(\text{OH})_2](A^{n-})_{x/n} \cdot m\text{H}_2\text{O}$ , where  $M^{2+}$  and  $M^{3+}$  are di- and trivalent metal cations, respectively, and  $A^{n-}$  is a counteranion.<sup>15</sup> The host structure

\* To whom correspondence should be addressed. Tel.: +86-10-64412131. Fax: +86-10-64425385. E-mail: weimin@mail.buct.edu.cn.

<sup>†</sup> Beijing University of Chemical Technology.

<sup>‡</sup> Nanjing University.

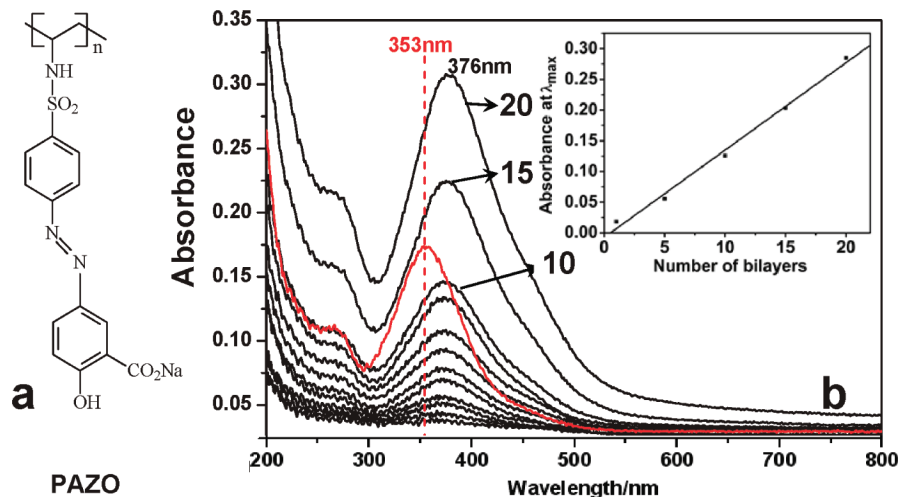


**Figure 1.** (a) The chemical structure of PAZO. (b) UV–visible absorption spectra of multilayer films of (LDH/PAZO)<sub>n</sub> assembled on a quartz glass substrate (“n” denotes the number of bilayers). The red line shows the spectrum of PAZO in aqueous solution. The absorbance of the films at  $\lambda_{\max}$  is plotted against the number of bilayers in the inset.

consists of brucite-like layers of edge-sharing  $M(\text{OH})_6$  octahedra, and the partial substitution of  $M^{3+}$  for  $M^{2+}$  results in positively charged host layers, balanced by the interlayer anions.<sup>16</sup> The preparation of LDH films is a fast-growing research field.<sup>17</sup> Owing to the pioneering work of Sasaki et al.,<sup>18</sup> much attention has been paid to the delamination of LDHs to obtain positively charged single nanosheets. One of the most important and attractive applications of such exfoliated nanosheets is that they serve as 2D building blocks to construct inorganic–organic ultrathin films with superior functionalities to those of either component alone. Therefore, the alternate LBL assembly of an azobenzene-containing polymer and LDH nanosheets can be expected to give rise to a new kind of photoresponsive film material. By providing the azobenzene chromophores with a rigid and ordered microenvironment, which eliminates the problem of interpenetration of polymer chains as well as the  $\pi$ – $\pi$  stacking interactions, the LDH layers should lead to enhanced photoresponsive performances.

In this work, we report the fabrication of hybrid ultrathin photoresponsive films based on LBL electrostatic self-assembly of positively charged LDH nanosheets and the negatively charged azobenzene-containing polymer 1-4[(3-carboxy-4-hydroxyphenylazo)benzenesulfonamido]-1,2-ethanediy] sodium salt, represented here as PAZO (Figure 1a). The photoisomerization of the films under alternate irradiation by UV and visible light is investigated experimentally, and the results are interpreted in terms of photoisomerization of PAZO in the matrix of LDH monolayer. Molecular dynamics (MD) studies have been carried out as a powerful supplementary technique to shed light on the isomerization process. It is anticipated that the strategy reported in this work can be employed to fabricate ultrathin films with interesting photochemical and photophysical properties based upon regular arrangements of organic chromophores within an inorganic matrix.

## Experimental Section

**Materials.** A colloidal suspension of exfoliated MgAl-LDH nanosheets with a lateral size of 2–4  $\mu\text{m}$  was synthesized by delamination of MgAl- $\text{NO}_3^-$ -LDH in formamide according to Sasaki’s process,<sup>18</sup> which we have employed in our previous work.<sup>19</sup> PAZO was purchased from Sigma-Aldrich and used without further purification. Deionized water with a conductance below  $10^{-6}$  S  $\text{cm}^{-1}$  was used during all the experiments. Quartz

slides with a thickness of 1.0 mm and Si wafers were used for film deposition. Quartz slides were used as substrates for the UV–visible absorption and polarized fluorescent spectroscopy, while Si wafers were used for AFM and SEM measurements.

**Fabrication of LDH/PAZO Multilayer Films.** Multilayer ultrathin films of LDH/PAZO were fabricated by applying the layer-by-layer assembly procedure. Substrates (silicon wafer or quartz glass slide) were immersed in a slightly boiled piranha solution (3:1 mixture of 98%  $\text{H}_2\text{SO}_4$  and 30%  $\text{H}_2\text{O}_2$ ) for 20 min, rinsed thoroughly with water, and dried at ambient temperature in a vacuum oven. A suspension of LDH nanosheets ( $1.0 \text{ g dm}^{-3}$ ) obtained as above was diluted with an equal volume of water. First, the freshly cleaned substrate was immersed in the colloidal suspension ( $0.5 \text{ g dm}^{-3}$ ) of LDH nanosheets for 10 min, which was followed by rinsing. Then the substrate was dipped in to a PAZO aqueous solution ( $1.0 \text{ g dm}^{-3}$ ) for 15 min and subsequently washed with water. Sequential deposition operations for LDH nanosheets and PAZO were repeated *n* times to produce multilayer films of (LDH/PAZO)<sub>n</sub>. The resulting films were finally dried at ambient temperature in a vacuum oven.

**Sample Characterization.** UV–visible absorption spectra were performed on a Shimadzu UV-2501PC spectrometer. The morphology and thickness of the (LDH/PAZO)<sub>n</sub> samples were investigated by using a Hitachi S-4700 SEM at an accelerating voltage of 20 kV. The surface topography of the (LDH/PAZO)<sub>n</sub> multilayer films deposited onto Si wafers before and after light illumination was examined using a NanoScope IIIa AFM from Veeco Instruments. A 500 W high-pressure mercury lamp and 300 W xenon lamp equipped with a filter ( $\lambda > 450 \text{ nm}$ ) were used as UV and visible light sources, respectively. The fluorescence polarization spectra were recorded on a QuantaMaster QM-4 spectrofluorometer, equipped with automated polarizers in both the excitation and the emission beams. A three-dimensional perspective for the experimental setup is provided in the Supporting Information (Scheme S1). The fluorescence spectra of the thin films were registered after excitation at 294 nm for (LDH/PAZO)<sub>n</sub> samples, where the fluorescence emission was collected along the Z-axis at  $90^\circ$  with respect to the excitation beam in the Z-axis. The spectra were scanned every 1 nm, with an integration time of 2 s, and excitation and emission slits of 8 nm. The orientation of the thin film with respect to the excitation beam was changed by

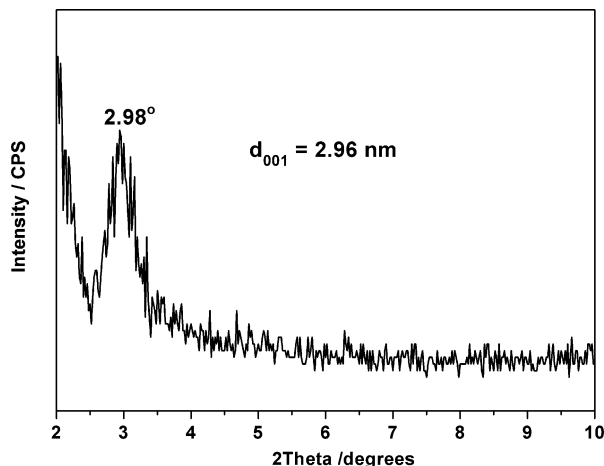


**Figure 2.** XRD pattern of the (LDH/PAZO)<sub>50</sub> film.

rotating the solid-sample holder around its vertical *y*-axis. The angle between the normal to the thin film and the excitation axis (defined as the angle  $\delta$  in Scheme S1) was scanned from 0° to 40°. The instrumental response to the linearly polarized light was corrected by recording the fluorescence signal of an isotropic system under identical experimental conditions. In this work, a  $2.5 \times 10^{-5}$  M aqueous solution of PAZO was used as the isotropic system.

**Theoretical Calculations.** Details for both the construction of the LDH/PAZO structural model and the molecular dynamics (MD) simulation on the isomerization of (LDH/PAZO)<sub>*n*</sub> films (Scheme S2) can be seen in the Supporting Information.

## Results and Discussion

**Film Fabrication.** Multilayer films were obtained by alternately dipping a quartz glass slide or silicon wafer into a colloidal suspension of the LDH nanosheets and PAZO solution. The multilayer buildup process of the film was monitored by UV–visible spectroscopy after each deposition cycle (shown in Figure 1b). The strong absorption band at approximately 376 nm is due to the (*A*<sub>1</sub>)  $\pi$ – $\pi^*$  transition in the *trans*-azobenzene isomer of PAZO. Compared with the absorption band at 353 nm of PAZO in aqueous solution (shown by the red line), the observed red shift may be attributed to the electrostatic interaction between LDH nanosheets and PAZO. As displayed in the inset of Figure 1b, the absorbance at 376 nm increases linearly with the number of bilayers, indicating a stepwise and regular film growth. The films also show a  $\Phi$ – $\Phi^*$  band near 250 nm (*A*<sub>s</sub>), which is attributed to a transition with electronic transition moment roughly parallel to the short axis of the *trans*-azobenzene chromophores.<sup>3b</sup> In contrast, the  $\pi$ – $\pi^*$  transition in the UV–visible spectra of the LDH/PAZO multilayer film at 376 nm is directed approximately along the long axis of *trans*-azobenzene chromophores. This makes it reasonable to expect that, in contrast to the  $\pi$ – $\pi^*$  transition, the  $\Phi$ – $\Phi^*$  transition of the aromatic cores is independent of the azobenzene orientation. As a result, the intensity ratio *A*<sub>s</sub>/*A*<sub>1</sub> can be used to evaluate the orientation of azobenzene group in the film.<sup>14d</sup> The *A*<sub>s</sub>/*A*<sub>1</sub> ratio for PAZO in aqueous solution was 0.61, which is representative of a random chromophore orientation. The *A*<sub>s</sub>/*A*<sub>1</sub> ratio for the LBL multilayer assembly was 0.76, which suggests that the rodlike chromophores exhibit a strong preference for an out-of-plane orientation with respect to the LDH layers. This will be further discussed in the next section.

The XRD pattern (Figure 2) for the (LDH/PAZO)<sub>50</sub> film illustrates a Bragg peak at  $2\theta = 2.98^\circ$ , indicating an average

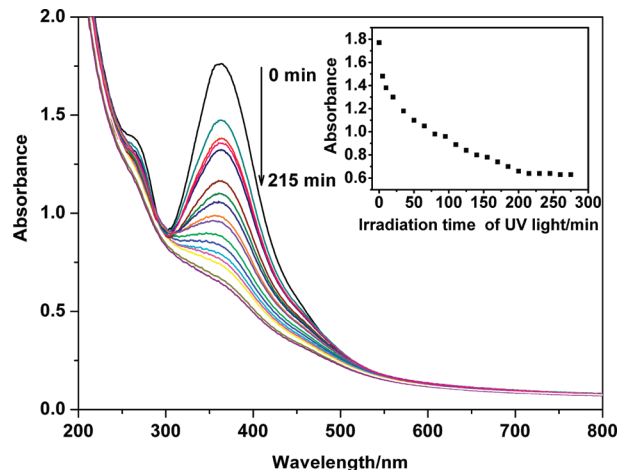


**Figure 3.** Variation in the UV–visible spectra of the (LDH/PAZO)<sub>50</sub> film with irradiation time by UV light. The inset shows the photoisomerization kinetics for the sample.

repeating distance of *ca.* 2.96 nm. This diffraction feature can be attributed to a so-called superlattice reflection of the inorganic/organic periodic nanostructure. Taking into account the thickness of  $\sim 0.48$  nm of the LDH nanosheet,<sup>18</sup> the height occupied by PAZO along the normal direction of the film was estimated to be  $\sim 2.5$  nm. This result indicates the ion exchange between PAZO polyanion and  $\text{NO}_3^-$  in the precursor LDH as well as the successful fabrication of the (LDH/PAZO)<sub>*n*</sub> film *via* electrostatic interaction between positively charged LDH nanosheets and negatively charged PAZO. The surface morphology and thickness of LDH/PAZO films were investigated by SEM. The top view of an SEM image (Supporting Information, Figure S1) for (LDH/PAZO)<sub>10</sub> shows the homogeneity of the film. The thickness of films with different bilayer numbers can be estimated by observing the corresponding side view SEM images (Supporting Information, Figure S2). As can be seen in Supporting Information, Figure S3, the thickness of the (LDH/PAZO)<sub>*n*</sub> film increases linearly with the increasing number of deposition cycles, with an average thickness increment of *ca.* 3.0 nm per deposition cycle, which is consistent with the result of XRD measurement. The film thickness increment of 3.0 nm per deposition cycle in this work is much larger than the typical values in multilayer films fabricated from alternative deposition of PAZO and positively charged polyelectrolytes.<sup>3b,14b</sup> The larger film thickness per cycle may be attributed to the intermeshing between adjacent polymer molecules being restrained by the isolating effect of the LDH nanosheets.

**Photoisomerization of (LDH/PAZO)<sub>*n*</sub> Multilayer Films.** It is interesting to evaluate the photoresponse of the LDH/PAZO multilayer films because *trans* to *cis* isomerization of azobenzene chromophores in condensed media depends significantly on the local environment such as polarity, viscosity, and free volume distribution around the chromophores. The photoisomerization reaction was studied by irradiating the sample with UV light and recording the absorption spectra at specific time intervals until a photostationary state was obtained. Figure 3 shows the change of UV–visible spectra of the (LDH/PAZO)<sub>50</sub> multilayer film during UV light illumination. As the photoisomerization reaction is induced by UV light there is a progressive decrease in the maximum intensity of  $\pi$ – $\pi^*$  band (*A*<sub>1</sub>). It was found that the equilibrium time (*t*<sub>equ</sub>) of *trans* to *cis* isomerization depends on the number of bilayers of LDH/PAZO (Supporting Information, Table S1). The kinetics of photoisomerization for the (LDH/PAZO)<sub>50</sub> film are shown in the inset of Figure 3. The best fit was obtained by simulating absorbance *A*(*t*) with an

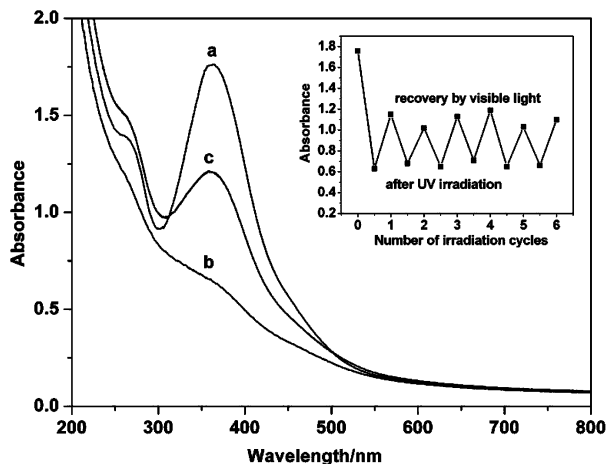


**Figure 4.** Photoisomerization of the (LDH/PAZO)<sub>50</sub> film. UV–visible absorption spectrum of the trans isomer (a), the same sample after irradiation with UV light (b), and of the recovered trans isomer after additional irradiation with visible light (c). The inset shows the change in the absorbance at the maximum of 376 nm upon alternate irradiation by UV and visible light.

initial exponential decay of the maximum absorbance  $A_1$ , with the following double exponential decay function:

$$A(t) = A_1 e^{-t/T_1} + A_2 e^{-t/T_2} + A_3 \quad (1)$$

The  $\pi$ – $\pi^*$  transition band (Figure 4a) nearly disappears after sufficient irradiation time (Figure 4b), indicating an almost complete trans to cis photochemical reaction. The  $\pi$ – $\pi^*$  absorption band increases again (Figure 4c) with irradiation by visible light ( $\lambda > 450$  nm), indicative of the cis–trans back-isomerization of azobenzene. Furthermore, reversible photochemical switching between the two isomers can be accomplished by alternate irradiation with UV and visible light, as shown in the inset of Figure 4. The extent of the cis to trans back-isomerization was estimated to be 51% from the change in the intensity of the  $\pi$ – $\pi^*$  transition band. During the photoisomerization processes, a significant change in film color can be observed (shown in Figure S4). These results demonstrate that the trans to cis isomerization reaction of the azobenzene chromophores in the (LDH/PAZO)<sub>n</sub> films is reversible and reproducible.

The high extent of trans to cis photoisomerization found in the (LDH/PAZO)<sub>n</sub> films suggests that the presence of the inorganic LDH nanosheets reduces both the intertwining of polymer chains and  $\pi$ – $\pi$  stacking of the azobenzene chromophores, and as a result sufficient free space is available for the isomerization of the azobenzene moiety. To illuminate the isolation effect introduced by the inorganic nanosheets, a pristine PAZO film sample was prepared using the drop-cast method as a comparison. After UV irradiation for 60 min, no photoisomerization behavior of the film was observed from the UV–visible absorption spectra (shown in Supporting Information, Figure S5). This indicates that the sufficient free volume afforded by incorporation of the LDH nanosheets is necessary for the photoisomerization of the azobenzene moiety. This will be further studied by molecular dynamics (MD) simulations as discussed below.

**Photoreorientation of Azobenzene Side Groups in (LDH/PAZO)<sub>n</sub> Multilayer Films.** The photoalignment of the azobenzene chromophores in the matrix of LDH nanosheets during the photoisomerization process was investigated by the fluorescence polarization method. The fluorescence spectra of the (LDH/PAZO)<sub>50</sub> film to horizontally (H) and vertically (V)

polarized incident light were recorded by varying the orientation angle  $\delta$  between the normal to the film and the incident light. A linear relationship between the fluorescence dichroic ratio ( $D_{HV}$  was defined as the ratio of H and V polarized emission spectra,  $D_{HV} = I_{HH}/I_{HV}$ ) and the twist angle  $\delta$  (with a right-angle configuration between the excitation and the emission beam) was established by means of<sup>20</sup>

$$(D_{HV})^{\text{cor}} = \frac{I_{HH}}{I_{HV}} G = 2 \cot^2 \psi + (1 - 2 \cot^2 \psi) \cos^2(90 + \delta) \quad (2)$$

where  $G$  is the instrumental  $G$  factor which makes a correction for the instrumental response to the emission H and V polarizer by taking into account the evolution of the fluorescence band of an isotropic system with the twist angles  $\delta$  recorded under identical conditions; that is,  $G \equiv (I_{HV}/I_{HH})^{\text{iso}}$ . An aqueous solution of PAZO was used as the isotropic system (see Experimental Section for further details). From the corresponding slope and/or intercept of a plot of  $(D_{HV})^{\text{cor}}$  versus  $\cos^2(90 + \delta)$ , the relative orientation of the interlayer azobenzene group can be evaluated in terms of the angle  $\psi$  (defined as the angle between the transition moment of azobenzene group and the normal to the LDH layer).

Figure 5 displays the fluorescence spectra of as-prepared (LDH/PAZO)<sub>50</sub> film recorded with the emission polarizer in the H ( $I_{HH}$ ) and V ( $I_{HV}$ ) directions for different twist angles  $\delta$ . The fluorescence intensity for the emission H polarizer increases when increasing the twist angle  $\delta$  from 0° up to 40° for the (LDH/PAZO)<sub>50</sub> ultrathin film. This confirms the fluorescence anisotropy of the multilayer film, which can be attributed to the preferential orientation of the interlayer azobenzene chromophores.

The evolution of the fluorescence dichroic ratio with the emission wavelength of the (LDH/PAZO)<sub>50</sub> ultrathin film for different twist angles  $\delta$  is shown in Figure 6. For a given  $\delta$  angle, the  $(D_{HV})^{\text{cor}}$  value is essentially independent of the emission wavelength, confirming the presence of only one type of PAZO species (monomer) for this sample. For a given emission wavelength, the dichroic ratio of the (LDH/PAZO)<sub>50</sub> film correlates linearly with the  $\cos^2(90 + \delta)$  value with a good correlation coefficient  $r = 0.9921$ , as shown in the inset of Figure 6 for the data measured at 420 nm. From the slope and intercept of the  $(D_{HV})^{\text{cor}}$  versus  $\cos^2(90 + \delta)$  linear relationship (eq 2), the orientation angle  $\psi$  of the transition moment of azobenzene with respect to the normal to the LDH layer was calculated to be 38° for the as-prepared (LDH/PAZO)<sub>50</sub> sample. Such an out-of-plane orientation of the azobenzene groups in the multilayer assembly is consistent with the UV–visible absorption spectra discussed above. The orientation of azobenzene groups in the film after UV light illumination and recovery under visible light were obtained in a similar way (Supporting Information, Figures S6, S7); the values of the angle  $\psi$  of the sample after UV light illumination and recovery are 62° and 44°, respectively. This indicates that the azobenzene chromophores in the matrix of LDH nanosheets undergo reversible photoalignment during the isomerization process, which will be further studied by molecular dynamics as discussed below.

**Morphological Change of the LBL Films Accompanied by Photoisomerization.** Figure 7 shows the AFM images of an (LDH/PAZO)<sub>10</sub> film on an Si wafer substrate during the complete photoisomerization process. Before UV illumination (Figure 7a), a large number of sharp peaks can be observed with a root-mean-square (rms) roughness of 7.8 nm, while the morphology changed drastically from sharp peaks to round

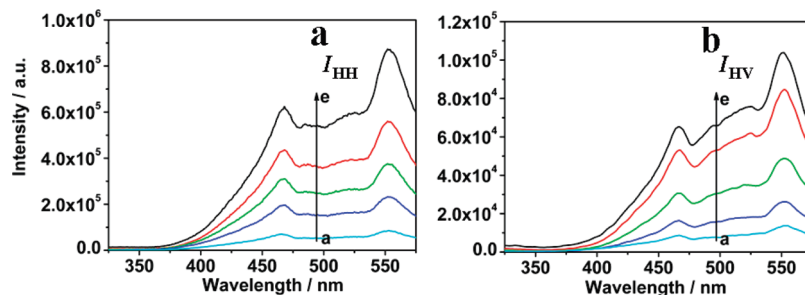


**Figure 5.** Evolution of the (a) H and (b) V polarized fluorescence spectra of the as-prepared (LDH/PAZO)<sub>50</sub> films with the following twist angles  $\delta$  of the sample: (a) 0, (b) 10, (c) 20, (d) 30, and (e) 40°. The spectra were recorded after excitation with horizontal polarized light.

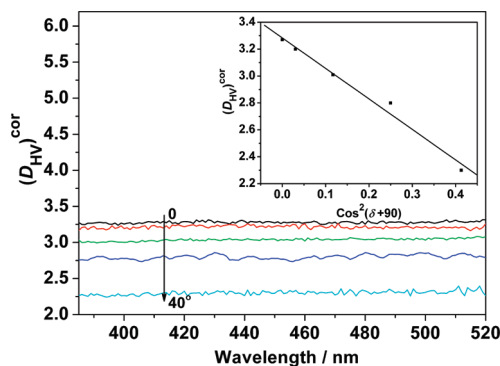


**Figure 6.** Evolution of the fluorescence dichroic ratio of the as-prepared (LDH/PAZO)<sub>50</sub> film with the emission wavelength for different twist angles  $\delta$  of the sample (see Figure 5 caption). The linear relationship between the dichroic ratio and  $\cos^2(\delta + 90)$  at 420 nm for the sample is included in the inset graph.

protuberances when the film was illuminated with UV light (Figure 7b), accompanied by a marked decrease in rms roughness (4.3 nm). After back-isomerization induced by visible light, a less smooth surface was observed with a rms roughness of 6.2 nm (Figure 7c). Molecular dynamics simulations<sup>20a,b</sup> have indicated that LDH host sheets are sufficiently flexible to deform around bulky intercalates such as DNA. On the basis these reports and the morphological changes of the film observed in this work, we propose a schematic illustration of the structural changes in the (LDH/PAZO)<sub>n</sub> film during the whole photoisomerization process (Scheme S3 in the Supporting Information). A number of islands on the surface of the LDH sheet result from its deformation induced by the deposited PAZO chain. Upon irradiation by UV light, the trans to cis photoisomerization gives rise to an increase in cross-sectional area but a decrease in the length of the long axis of the azobenzene chromophores.<sup>21</sup> This leads to the increase in diameter and decrease in height of the islands. However, the cis to trans isomerization of the azobenzene group induced by visible light results in the converse morphological change owing to the recovery of the original geometric shape of azobenzene.

**Simulation of the Isomerization Process of PAZO/LDH. Trans to Cis Isomerization of PAZO between the LDH Monolayers.** Figure 8 shows four typical snapshots during the trans to cis isomerization. It was observed that the  $t_{1/2}$  and reaction time from trans- to cis-PAZO are 55 and 135 fs, respectively. Additionally, the interlayer spacing of the PAZO/LDH film initially increased slightly (from 35.74 Å to 35.88 Å), and then decreased during the trans to cis isomerization process (33.11 Å), implying that the initial enlargement of the interlayer spacing may be a key factor in the occurrence of this trans to cis isomerization process.

#### *cis*-PAZO to (50% *cis* + 50% *trans*)-PAZO Isomerization

**between the LDH Monolayers.** When the back-isomerization of *cis*-PAZO to (50% *cis* + 50% *trans*)-PAZO occurs (shown in Figure 9), it was found that the interlayer spacing increases from 31.96 to 33.45 Å over the whole time range. The reaction time is ca. 85 fs, which is longer than the  $t_{1/2}$  value for *trans*- to *cis*-PAZO isomerization. This indicates that the recovery process is more difficult than the trans to cis isomerization. This can be explained by the resistance to expansion of the interlayer spacing which must be overcome on going from *cis*- to *trans*-PAZO/LDH. The discussion on interlayer spacing changes and diffusion properties of PAZO between the LDH nanosheets can be seen in the Supporting Information.

**Reversible Photoalignment of Azobenzene between the LDH Monolayers.** To further understand the orientation of azobenzene groups in PAZO confined between the LDH monolayers during the isomerization process, three orientation angles were defined to describe the geometries of the azobenzene group (shown in Figure 10):  $\theta_1$  stands for the angle between the benzene ring attached to the carboxyl group and the LDH monolayer;  $\theta_2$  stands for the angle between the transition moment direction of PAZO (the long axis direction of azobenzene for *trans*-PAZO and the N=N direction for *cis*-PAZO and (50% *cis* + 50% *trans*)-PAZO) with respect to the LDH monolayer;  $\theta_3$  represents the C–N=N–C torsion angle. Figure 11a displays the distribution of  $\theta_1$  for three typical states. The distributions of angle  $\theta_1$  for these states are mainly populated in the range from 0° to 65°. For the LDH/*trans*-PAZO, the most probable angle  $\theta_1$  is 30°. As the configuration of azobenzene changes from trans to cis,  $\theta_1$  moves to the low angle region and is mainly distributed at ca. 15°. Moreover, for the LDH/(50% *cis* + 50% *trans*)-PAZO state,  $\theta_1$  moves back to the higher angle region with a most probable angle of ca. 25°. It thus can be concluded that the orientation of azobenzene in PAZO changes from tilted to nearly horizontal relative to the LDH layer when the trans to cis isomerization occurs. Angle  $\theta_2$ , which is related to the transition moment direction of azobenzene in the gallery of LDH, is illustrated in Figure 11b. It was found that the most probable values of  $\theta_2$  are 68°, 36°, and 54° for the LDH/*trans*-PAZO, LDH/*cis*-PAZO, and LDH/(50% *cis* + 50% *trans*)-PAZO state, respectively, demonstrating that the N=N bond shifts from a vertical to a tilted arrangement with respect to the monolayer on changing from the trans isomer to the cis isomer. Furthermore, based on the relationship  $\theta_2 + \psi = 90^\circ$ , the variation in  $\theta_2$  is in reasonable agreement with that of orientation angle  $\psi$  (shown in Figure 10) as determined by fluorescence polarization measurements (values of  $\psi$  are 38° for the trans isomer, 62° for the cis isomer and 44° for the LDH/(50% *cis* + 50% *trans*)-PAZO), although some differences between the experimental and computational values do exist. The absolute value of the C–N=N–C torsion angle ( $\theta_3$ ) is an important parameter in determining the trans and cis structures

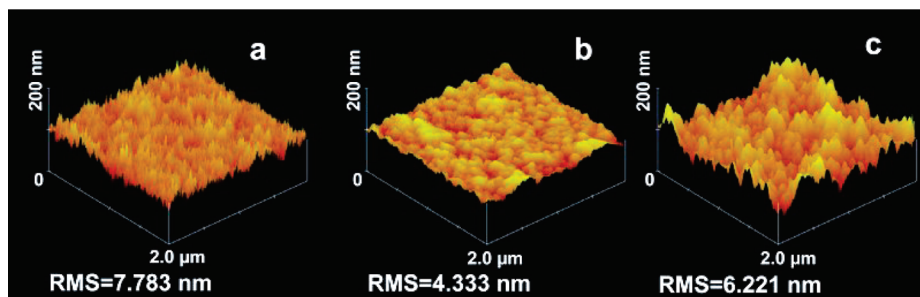


**Figure 7.** AFM images of an LBL film of (LDH/PAZO)<sub>10</sub> on an Si wafer substrate (a) before and (b) after illumination with UV light and (c) after subsequent illumination with visible light.

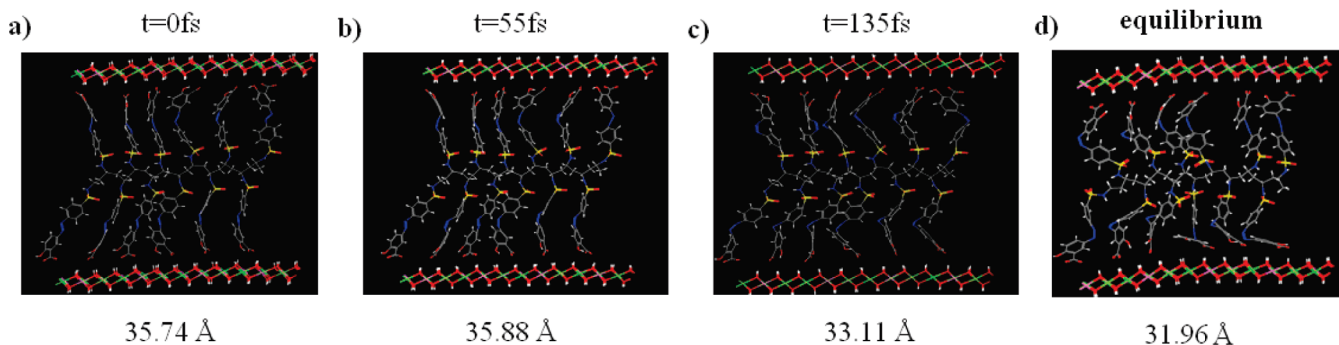


**Figure 8.** Snapshots of the trans to cis isomerization process of PAZO: (a) LDH/*trans*-PAZO, (b) LDH/(50% *trans* + 50% *cis*)-PAZO, (c) LDH/*cis*-PAZO, (d) the equilibrium state of LDH/*cis*-PAZO.

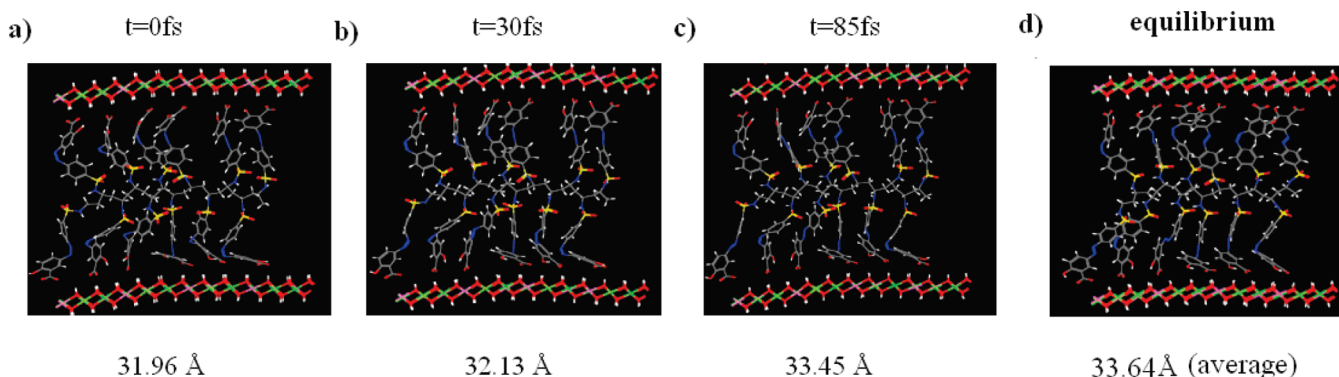


**Figure 9.** Snapshots of the cis to trans isomerization process of PAZO: (a) LDH/*cis*-PAZO, (b) LDH/(75% *cis* + 25% *trans*)-PAZO, (c) LDH/(50% *cis* + 50% *trans*)-PAZO, (d) the equilibrium state of LDH/(50% *cis* + 50% *trans*)-PAZO.

(shown in Figure 11c). It can be observed that angle  $|\theta_3|$  is mainly distributed from 130 to 180° with the most probable angle of 160° for the LDH/*trans*-PAZO system, while for LDH/*cis*-PAZO  $|\theta_3|$  is populated in the range 0–30° with the most probable angle of 0°. Moreover, both of the two angles (160° and 0°) can be observed with nearly symmetrical distribution for the LDH/(50% *cis* + 50% *trans*)-PAZO as expected.

## Conclusion

In summary, we demonstrate the photoswitching properties of (LDH/PAZO)<sub>n</sub> multilayer films in which azobenzene chromophores exhibit reversible *trans*–*cis* photoisomerization. The isolation effect of LDH nanosheets imposes enough free volume for the photoisomerization of the azobenzene group in PAZO, accounting for its complete *trans* to *cis* isomerization as well as high reversibility and reproducibility. This has been further confirmed by MD simulation studies. Both the fluorescence polarization technique and MD simulations demonstrate the reversible photoalignment of the azobenzene group during the photoisomerization process, providing a detailed understanding

of the configurational and orientational variation for the *trans* to *cis* isomerization of azobenzene in PAZO. A reversible surface morphological change of the LBL film induced by alternate UV and visible light was observed by AFM, corresponding to the variation in interlayer distance as well as the flexibility of LDH nanosheets revealed by MD studies. Therefore, this work provides an attractive and feasible methodology for the fabrication of light-sensitive films with photochemical switching properties. Furthermore, by virtue of the highly tunable compositions for both the inorganic and organic parts, these multilayer films can be potentially applied in the fields of optical coatings, photosensors, and optical information storage.

**Acknowledgment.** This project was supported by the National Natural Science Foundation of China, the 111 Project (Grant No. B07004), the 973 Program (Grant No. 2009CB939802), and the Fundamental Research Funds for the Central Universities (Grant No. ZZ0908).

**Supporting Information Available:** Molecular dynamic simulation details; SEM images (Figures S1, S2); the thickness

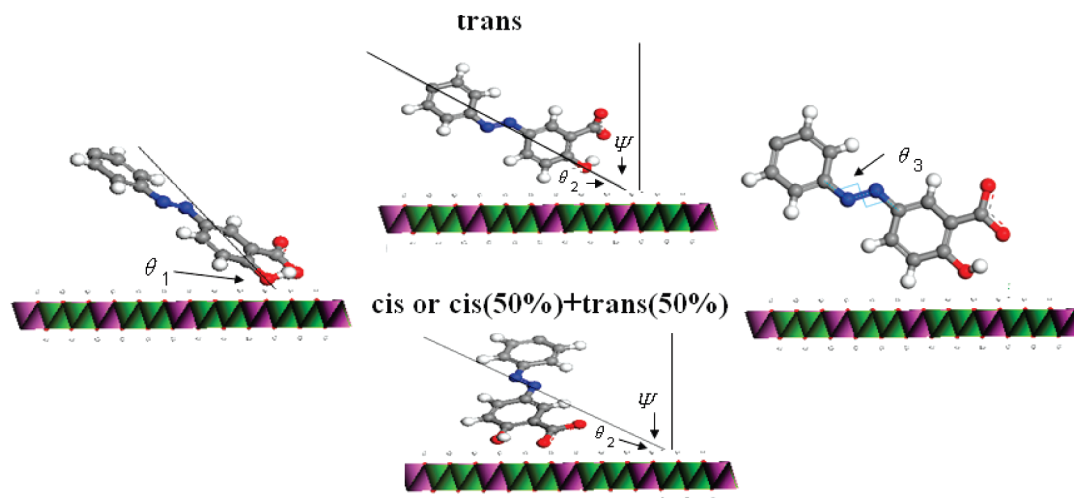


**Figure 10.** Definitions for the three orientation angles of azobenzene group in the gallery of LDH.

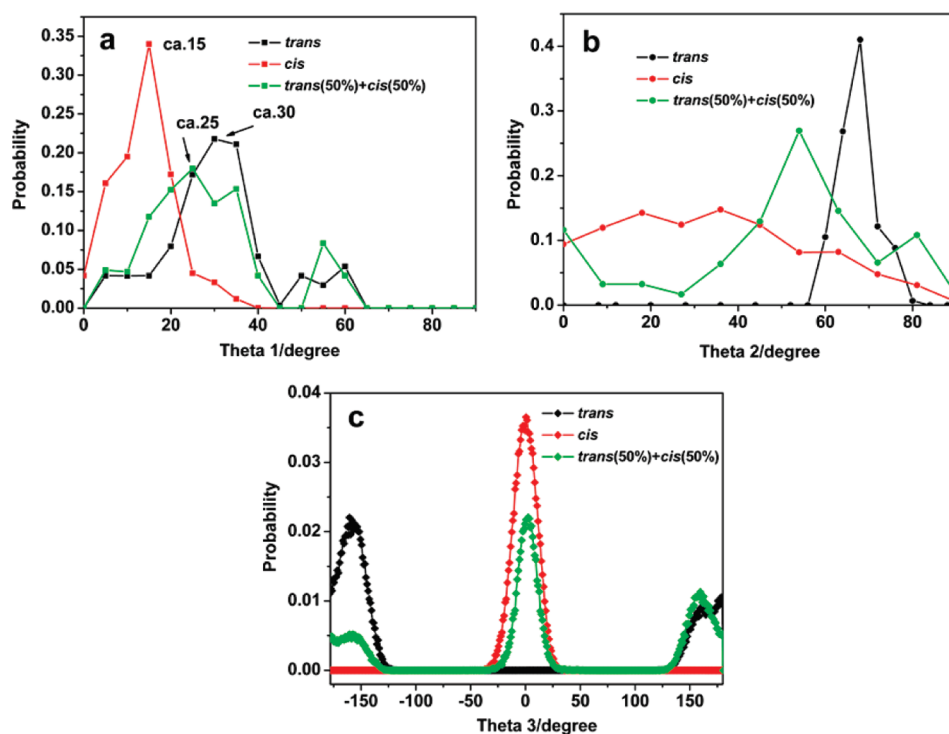


**Figure 11.** The distribution of the orientation angles for the three configurations in the LDH/PAZO system: (a)  $\theta_1$ , (b)  $\theta_2$ , (c)  $\theta_3$ .

of (LDH/PAZO)<sub>n</sub> multilayer films as a function of number of bilayers (Figure S3); photograph of the (LDH/PAZO)<sub>50</sub> film during the photoisomerization process (Figure S4); UV–visible spectra of the PAZO film as-prepared by the drop-casting method and after UV irradiation for 60 min (Figure S5); polarized fluorescence spectra and fluorescence dichroic ratio of the film for different twisting  $\delta$  angles after UV irradiation and cis to trans recovery (Figures S6, S7); mean square displacements (MSD) of the azobenzene group in PAZO molecules as a function of time at 298 K (Figure S8); three-dimensional perspective for the experimental setup to record polarized fluorescence spectra (Scheme S1); structural models for Mg–Al–LDH and anionic *trans*-PAZO (Scheme S2); a schematic model of the structural change of (LDH/PAZO)<sub>n</sub> films accompanied by photoisomerization (Scheme S3); the distortion of the LDH layer during the simulations (Scheme S4); the equilibrium time ( $t_{\text{equ}}$ ) of trans to cis photoisomerization of (LDH/PAZO)<sub>n</sub> films with different bilayer numbers (Table S1); self-diffusion coefficients of azobenzene in PAZO molecules

(Table S2). This material is available free of charge via the Internet at <http://pubs.acs.org>.

## References and Notes

- (1) (a) Ludwig, S.; Bayley, H. *J. Am. Chem. Soc.* **2006**, *128*, 12404. (b) Natansohn, A.; Rochon, P. *Chem. Rev.* **2002**, *102*, 4139. (c) Francesca, S.; Eugene, M. T. *Macromolecules* **2008**, *41*, 981.
- (2) (a) Thomas, F.; Joachim, H.; Wendorff, D. J.; Vasile, C. *Chem. Mater.* **2003**, *15*, 2146. (b) Ikeda, T.; Tsutsumi, O. *Science* **1995**, *268*, 1873. (c) Astrand, P.-O.; Ramanujam, P. S.; Hvilsted, S.; Bak, K. L.; Sauer, S. P. A. *J. Am. Chem. Soc.* **2000**, *122*, 3482.
- (3) (a) Puntoriero, F.; Ceroni, P.; Balzani, V.; Bergamini, G.; Vögtle, F. *J. Am. Chem. Soc.* **2007**, *129*, 10714. (b) Dante, S.; Advincula, R.; Frank, C. W.; Stroeve, P. *Langmuir* **1999**, *15*, 193. (c) Seiji, K.; Syugo, N.; Takamasa, N. *Chem. Mater.* **2000**, *12*, 9.
- (4) (a) Gunnlaugsson, T.; Leonard, J. P.; Murray, N. S. *Org. Lett.* **2004**, *6*, 1557. (b) Mermut, O.; Barrett, C. J. *Analyst* **2001**, *11*, 1861. (c) Bradford, A.; Drake, P. L.; Worsfold, O.; Peterson, I. R.; Walton, D. J.; Price, G. J. *Phys. Chem. Chem. Phys.* **2001**, *9*, 1750.
- (5) (a) Feng, C. L.; Zhang, Y. J.; Jin, J.; Song, Y. L.; Xie, L. Y.; Qu, G. R.; Jiang, L.; Zhu, D. B. *Langmuir* **2001**, *17*, 4593. (b) Ichimura, K.;

Oh, S. K.; Nakagawa, M. *Science* **2000**, *288*, 1624. (c) Oh, S. K.; Nakagawa, M.; Ichimura, K. *J. Mater. Chem.* **2002**, *12*, 2262.

(6) (a) Han, M.; Ichimura, K. *Macromolecules* **2001**, *34*, 82. (b) Eich, M.; Wendroff, J. H.; Beck, B.; Ringsdorf, H. *Macromol. Chem. Rapid Commun.* **1987**, *8*, 59. (c) Nobuyuki, T.; Yasuyuki, A.; Masaya, M.; Masatoshi, K. *Chem. Mater.* **2003**, *15*, 719.

(7) (a) Neff, G. A.; Helfrich, M. R.; Clifton, M. C.; Page, C. J. *Chem. Mater.* **2000**, *12*, 2363. (b) Kang, E. H.; Bu, T. J.; Jin, P. C.; Sun, J. Q.; Yang, Y. Q.; Shen, J. C. *Langmuir* **2007**, *23*, 7594. (c) Casson, J. L.; McBranch, D. W.; Robinson, J. M.; Wang, H. L.; Roberts, J. B.; Chiarelli, P. A.; Johal, M. S. *J. Phys. Chem. B* **2000**, *104*, 11996.

(8) (a) Creatini, L.; Cusati, T.; Granucci, G.; Persico, M. *Chem. Phys.* **2008**, *347*, 492. (b) Wu, L. F.; Tuo, X. L.; Cheng, H.; Chen, Z.; Wang, X. G. *Macromolecules* **2001**, *34*, 8005. (c) Song, X.; Perlstein, J.; Whitten, D. G. *J. Am. Chem. Soc.* **1997**, *119*, 9144. (d) Santos, D. S., Jr.; Mendonca, C. R.; Balogh, D. T.; Dhanabalan, A.; Cavalli, A.; Misoguti, L.; Giacometti, J. A.; Zilio, S. C.; Oliveira, O. N., Jr. *Chem. Phys. Lett.* **2000**, *317*, 1.

(9) (a) Wang, Y. P.; Ma, N.; Wang, Z. Q.; Zhang, X. *Angew. Chem., Int. Ed.* **2007**, *46*, 2823. (b) Sanchez, A. M.; Rossi, R. H. *J. Org. Chem.* **1996**, *61*, 3446. (c) Douhal, A. *Chem. Rev.* **2004**, *104*, 1955.

(10) (a) Badjic, J. D.; Kostic, N. M. *J. Phys. Chem. B* **2001**, *105*, 7482. (b) Ma, N.; Wang, Y. P.; Wang, B. Y.; Wang, Z. Q.; Zhang, X. *Langmuir* **2007**, *23*, 2874.

(11) (a) Ogawa, M.; Ishii, T.; Miyamoto, N.; Kuroda, K. *Adv. Mater.* **2001**, *13*, 1107. (b) Tong, Z. W.; Sasamoto, S.; Shimada, T.; Takagi, S.; Tachibana, H.; Zhang, X. B.; Tryk, D. A.; Inoue, H. *J. Mater. Chem.* **2008**, *18*, 4641. (c) Costantino, U.; Nocchetti, M.; Vivani, R. *J. Am. Chem. Soc.* **2002**, *124*, 8428. (d) Gentili, P. L.; Costantino, U.; Vivani, R.; Latterini, L.; Nocchetti, M.; Aloisi, G. G. *J. Mater. Chem.* **2004**, *14*, 1656.

(12) (a) Mi-Jeong, K.; Eun-Mi, S.; Doojin, V.; Dong-Yu, K. *Chem. Mater.* **2003**, *15*, 4021. (b) Chiarelli, P. A.; Johal, M. S.; Holmes, D. J.; Casson, J. L.; Robinson, J. M.; Wang, H.-L. *Langmuir* **2002**, *18*, 168.

(13) (a) Robert, A. H.; Masahiko, H.; Wolfgang, K. *Langmuir* **1996**, *12*, 2551. (b) Liu, Z. F.; Zhao, C. X.; Tang, M.; Cai, S. M. *J. Phys. Chem.* **1996**, *100*, 17337. (c) Takashi, Y.; Yasushi, U.; Osamu, S.; Yasuaki, E. *Chem. Mater.* **2004**, *16*, 1195.

(14) (a) Toutianoush, A.; Tieke, B. *Macromol. Rapid Commun.* **1998**, *19*, 591. (b) Mermut, D.; Barrett, C. J. *J. Phys. Chem. B* **2003**, *107*, 2525.

(c) Hong, J. D.; Park, E. S.; Park, A. L. *Langmuir* **1999**, *15*, 6515. (d) Kumar, S. K.; Hong, J. D.; Lim, C. K.; Park, S. Y. *Macromolecules* **2006**, *39*, 3217.

(15) (a) Williams, G. R.; O'Hare, D. *J. Mater. Chem.* **2006**, *16*, 3065. (b) Gursky, J. A.; Blough, S. D.; Luna, C.; Gomez, C.; Luevano, A. N.; Gardner, E. A. *J. Am. Chem. Soc.* **2006**, *128*, 8376. (c) Desigaux, L.; Belkacem, M. B.; Richard, P.; Cellier, J.; Lone, P.; Cario, L.; Leroux, F.; Taviot-Guého, C.; Pitard, B. *Nano Lett.* **2006**, *6*, 199. (d) Hou, X. Q.; Kirkpatrick, R. J. *Chem. Mater.* **2002**, *14*, 1195. (e) Xu, Z. P.; Braterman, P. S.; Yu, K.; Xu, H. F.; Wang, Y. F.; Brinker, C. J. *Chem. Mater.* **2004**, *16*, 2750.

(16) (a) Darder, M.; Blanco, M. L.; Aranda, P.; Leroux, F.; Hitzky, E. R. *Chem. Mater.* **2005**, *17*, 1969. (b) Richardson, M. C.; Braterman, P. S. *J. Phys. Chem. C* **2007**, *111*, 4209. (c) Hou, X. Q.; Kirkpatrick, R. J. *Inorg. Chem.* **2001**, *40*, 6397. (d) Khan, A. I.; Lei, L. X.; Norquist, A. J.; O'Hare, D. *Chem. Commun.* **2001**, *1*, 2342. (e) Gardner, E. A.; Huntoon, K. M.; Pinnavaia, T. J. *Adv. Mater.* **2001**, *13*, 1263.

(17) (a) Lee, J. H.; Rhee, S. W.; Nam, H. J.; Jung, D.-Y. *Adv. Mater.* **2008**, *20*, 1. (b) Han, E.; Shan, D.; Xue, H. G.; Cosnier, S. *Biomacromolecules* **2007**, *8*, 971. (c) Yarger, M. S.; Steinmiller, E. M. P.; Choi, K.-S. *Inorg. Chem.* **2008**, *47*, 5859. (d) Iyi, N.; Ebina, Y.; Sasaki, T. *Langmuir* **2008**, *24*, 5591. (e) Scavetta, E.; Ballarin, B.; Gazzano, M.; Tonelli, D. *Electrochim. Acta* **2009**, *54*, 1027. (f) Yan, D. P.; Lu, J.; Wei, M.; Han, J. B.; Ma, J.; Li, F.; Evans, D. G.; Duan, X. *Angew. Chem., Int. Ed.* **2009**, *48*, 3073.

(18) (a) Li, L.; Ma, R. Z.; Ebina, Y.; Iyi, N.; Sasaki, T. *Chem. Mater.* **2005**, *17*, 4386. (b) Liu, Z. P.; Ma, R. Z.; Osada, M.; Iyi, N.; Ebina, Y.; Takada, K.; Sasaki, T. *J. Am. Chem. Soc.* **2006**, *128*, 4872. (c) Li, L.; Ma, R. Z.; Ebina, Y.; Fukuda, K.; Sasaki, T. *J. Am. Chem. Soc.* **2007**, *129*, 8000.

(19) Han, J. B.; Lu, J.; Wei, M.; Wang, Z. L.; Duan, X. *Chem. Commun.* **2008**, *41*, 5188.

(20) (a) López Arbeloa, F.; Martínez Martínez, V. *Chem. Mater.* **2006**, *18*, 1407. (b) López Arbeloa, F.; Martínez Martínez, V. *J. Photochem. Photobiol. A: Chem.* **2006**, *181*, 44.

(21) (a) Matsumoto, M.; Miyazaki, D.; Tanaka, M.; Azumi, R.; Manda, E.; Kondo, Y.; Yoshino, N.; Tachibana, H. *J. Am. Chem. Soc.* **1998**, *120*, 147. (b) Sasaki, Y. C.; Suzuki, Y.; Tomioka, Y.; Ishibashi, T.; Takahashi, M.; Satoh, I. *Langmuir* **1996**, *12*, 4173.

JP9114018